Evaluation of ERA-Interim for Tropospheric Delay and Water Vapor Estimation in Different Climate Zones using Ground-based GNSS Observations

EGU2017–19456

Furqan Ahmed[1,2], Addisu Hunegnaw[2], Norman Teferle[2], and Richard Bingley[3]

(1) Center for Space Research, University of Texas at Austin, USA
(2) Institute of Geodesy and Geophysics, University of Luxembourg, Luxembourg
(3) Nottingham Geospatial Institute, University of Nottingham, UK

Contact: furqan.ahmed@csr.utexas.edu

Abstract

Tropospheric delay and integrated water vapor (IWV) derived from climate reanalysis models, such as that of the European Centre for Medium-range Weather Forecasts (ECMWF) namely the ECMWF ReAnalysis-Interim (ERA-Interim), are widely used in many geodetic and atmospheric applications. Therefore, it is of interest to assess the quality of these reanalysis products using available observations. Observations from Global Navigation Satellite Systems (GNSS) are, as of now, available for a period of over 2 decades and their global availability make it possible to validate the zenith total delay (ZTD) and IWV obtained from climate reanalysis models in different geographical and climatic regions. In this study, a 5-year long homogeneously reprocessed GNSS data set based on a double difference positioning strategy and containing over 400 globally distributed ground-based GNSS stations has been used as a reference to validate the ZTD estimates obtained from the ERA-Interim climate reanalysis model in 25 different climate zones. It has been studied how the difference between the ERA-Interim ZTD and the GNSS-derived ZTD varies with respect to the different climate zones as well as the topographic variations in a particular climate zone. Periodicity in the ZTD residuals in different climate zones has been analyzed. Furthermore, the variation of the ZTD differences with respect to latitude has been presented. Finally, for one GNSS station in each of the 25 climate zones, IWV derived from ERA-Interim has been compared to the IWV derived using GNSS observations.

Introduction

Climate reanalysis datasets, such as the ECMWF ERA-Interim, provide global gridded values of several atmospheric variables with uniform spatial and temporal resolutions and time spans of three decades or more in the past. These values are obtained using a consistent and stable assimilation of observations over the whole time span. Hence, there is an opportunity to use the climate reanalysis values at the spatial and temporal points where the observations are not available. Furthermore, for several geodetic techniques, climate reanalysis models are also used to model the atmospheric effects (e.g. tropospheric mapping functions). Therefore, it is important to study if the performance of the climate reanalysis models depends on the geographical and climatic properties of the region of interest.

In this study, the ZTD and IWV derived using meteorological values from ERA-Interim have been compared to the ZTD and IWV values derived using GNSS observations. Furthermore, the differences between the ERA-Interim and GNSS datasets have been discussed in reference to climatic and geographical properties.

The classification of climate types used here is the one given by Peel et al. (2007) as an updated version of the Köppen-Geiger climate classification that consists of 30 climate types. Combination of all the regions with a specific climate type is referred to as a "climate zone". A climate zone can be denoted by a string of two to three characters (case sensitive) where the meaning of each character in parenthesis is given in Table 1.

Table 1. Characters used to denote different climate zones with their meanings (Note: there is no relation between the individual rows of this table)

1st Character:	A (Tropical)	B (Arid)	C (Temperate)	D (Cold)	E (Polar)			
2nd Character:	f (Rainforest)	m (Monsoon)	s (Dry Summer)	w (Savannah)	S (Steppe)	W (Desert)	F (Frost)	T (Tundra)
3rd Character:	a (Hot Summer)	b (Warm Summer)	c (Cold Summer)	d (Very Cold Winter)	h (Hot)	k (Cold)		

A network of over 400 globally distributed ground-based GNSS stations has been processed with the characteristics shown in Table 2 to obtain the ZTD. The processed stations have further been designated to their respective climate zones. Figure 1 shows the global distribution of GNSS stations with respect to the various climate zones using color-, and symbol-coding. Figure 2 shows the number of processed GNSS stations in each climate zone.

Table 2. Processing characteristics of the GNSS ZTD dataset

Parameter	Value
Processing Strategy	Double Difference Positioning
Processing Software	BSW52
ZTD Output Interval	2 hours
Observation Window Length	24 hours
Processing Session Length	24 hours
GNSS Used	GPS
A-Priori Coordinates	PPP
A-Priori ZHD Model	Dry VMF1
Tropospheric Mapping Function	Wet VMF1
Orbit Product Used	COD Repro1
Clock Product Used	COD Repro1
Antenna Models	IGS08
Elevation Cut-Off Angle	3°
Integer Ambiguity Resolution	Yes
Ocean Tide Loading Correction	FES2004
Reference Frame Standard	IERS2010
Ionosphere Correction	1st and 2nd Order

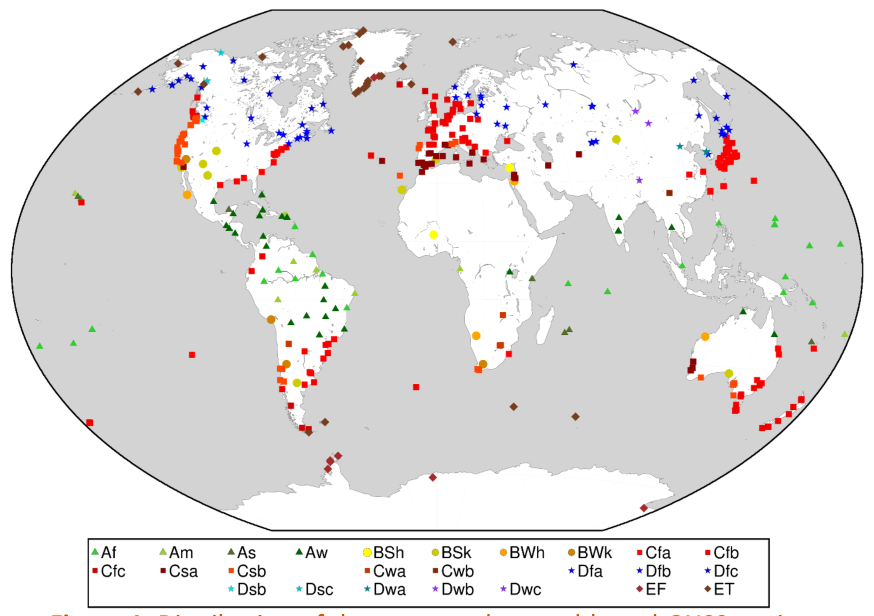

Figure 1. Distribution of the processed ground-based GNSS stations with respect to climate zones

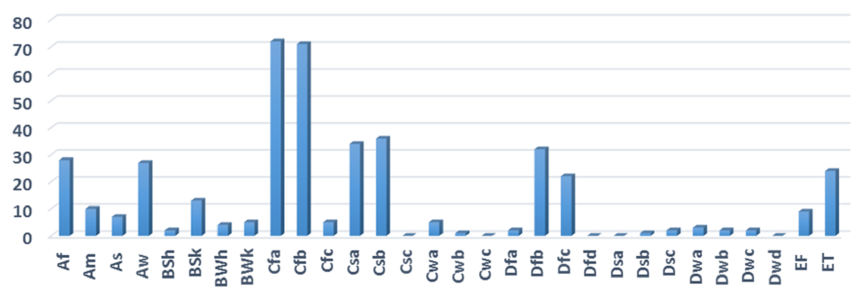

Figure 2. Number of GNSS stations in different climate zones

ERA-Interim ZTD at the GNSS station coordinates has been obtained using the GOP-TropDB online service of the Geodetic Observatory Pecny (http://www.pecny.cz/gop/index.php/gop-tropdb/tropo-model-service). A comparison has been performed between the GNSS-derived ZTD (ZTD_{gnss}) and ERA-Interim ZTD (ZTD_{erai}) for all the stations using 5 years of data and the original temporal resolution of ERA-Interim i.e. 6-hours.

ZTD Comparison Results

In the ZTD dataset used for this study, processed ground-based GNSS stations were available for 25 out of the 30 climate zones mentioned in the previous section. Therefore, this study is based on 25 climate zones. For the ease of notation, we denote the difference between ZTD_{erai} and ZTD_{gnss} by ΔZTD in the following text (i.e. $\Delta ZTD = ZTD_{erai} - ZTD_{gnss}$). Overall, the correlation coefficient between ZTD_{erai} and ZTD_{gnss} (r_{ztd}) ranges from 0.87 to 1.00. The mean, standard deviation and RMS of ΔZTD range from -4.49 to 15.31 mm, 0.08 to 21.06 mm and 1.64 to 22.72 mm, respectively. Table 3 shows the statistics for ΔZTD for the 25 analyzed climate zones. The highest values of r_{ztd} (1.00 and 0.99) have been found for the "Cold (D)", whereas the lowest values of r_{ztd} (0.87 and 0.88) have been found for "Tropical (A)" climate zones.

Table 3. Statistics of ΔZTD for different climate zones

Zone	Mean [mm]	SDev. [mm]	RMS [mm]	r_{ztd}
Af	-2.25	8.92	9.20	0.87
Am	-2.56	5.65	6.20	0.87
As	-4.49	7.37	8.63	0.88
Aw	2.25	10.32	10.56	0.88
BSh	3.54	4.24	5.53	0.92
BSk	0.30	5.25	5.26	0.91
BWh	-0.41	4.42	4.44	0.94
BWk	10.42	11.10	15.23	0.92
Cfa	2.33	6.00	6.43	0.96
Cfb	1.06	6.39	6.47	0.93
Cfc	5.90	3.65	6.94	0.96
Csa	4.53	7.78	9.00	0.90
Csb	3.76	4.03	5.51	0.91
Cwa	8.53	21.06	22.72	0.97
Cwb	1.79	17.44	17.54	0.89
Dfa	-0.79	2.65	2.76	0.95
Dfb	2.19	5.97	6.36	0.98
Dfc	2.25	6.13	6.53	0.99
Dsb	15.31	15.23	21.59	0.95
Dsc	-1.63	0.08	1.64	1.00
Dwa	-0.39	2.80	2.83	1.00
Dwb	6.04	7.00	9.25	0.99
Dwc	6.33	2.11	6.67	1.00
EF	-0.41	2.43	2.47	0.95
ET	3.58	5.04	6.18	0.98

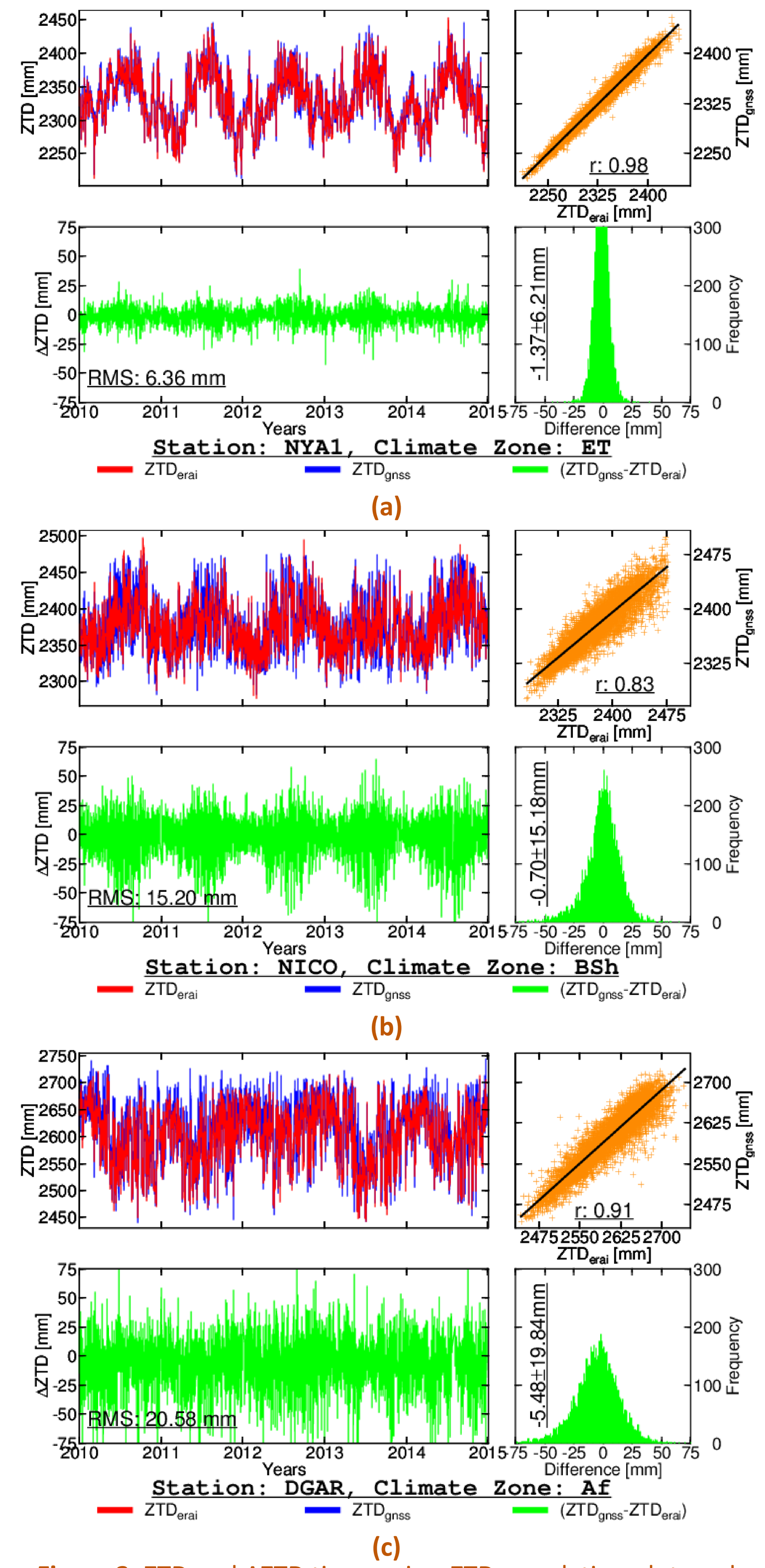

Figure 3. ZTD and ΔZTD time series, ZTD correlation plot, and ΔZTD histogram for stations a) NYA1, b) NICO and c) DGAR

Figure 3 shows the comparison of ZTD_{erai} and ZTD_{gnss} in the form of ZTD and ΔZTD time series, correlation plots and histograms, for three randomly selected stations as examples. Among the three stations shown by Figure 3, the station in the Polar climate type (NYA1) can be seen to have better agreement between ZTD_{erai} and ZTD_{gnss} in contrast to the stations in Tropical (DGAR) and Arid (NICO) locations. This fact indicates towards a relationship between the amount of atmospheric water vapor in a climate zone and ΔZTD.

The difference between ZTD_{erai} and ZTD_{gnss} has also been studied in relation to latitude. Figure 4 shows the global distribution, as well as the distribution with respect to latitude, of r_{ztd} and RMS(ΔZTD). It can be seen from Figure 4 that the two ZTD datasets agree better near the polar regions.

The topographic properties (in terms of minimum, maximum and average ellipsoidal heights of GNSS stations) for all the climate zones were collected and their relationship to ΔZTD was studied. It was found that the highest mean, standard deviation and RMS of ΔZTD correspond to the climate zones with high altitude and high topographic variation.

Furthermore, periodicity in the time series of ΔZTD was computed for one GNSS station in each climate zone and it was found that the periodic behavior of ΔZTD is different in different climate zones and higher periodicity leads to higher difference.

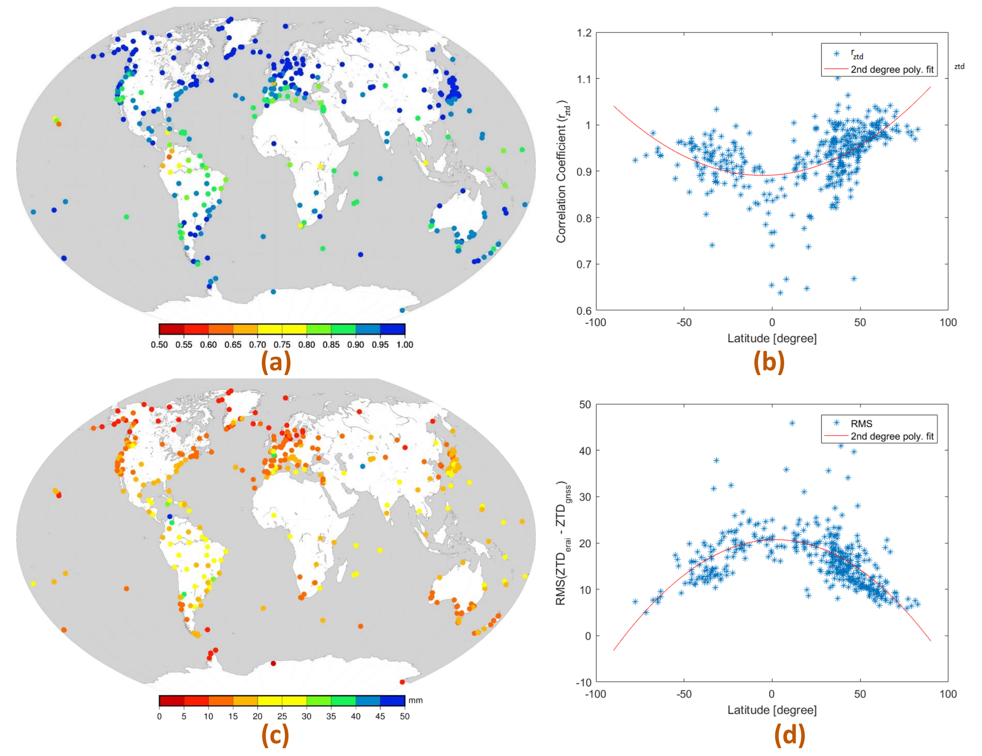

Figure 4. Global distributions of r_{ztd} (a) and RMS(ΔZTD) (b), and latitude-wise distribution of r_{ztd} (b) and RMS(ΔZTD) (d)

IWV Comparison Results

For one GNSS station in each of the 25 analyzed climate zones, ZTD_{gnss} was converted to IWV_{gnss} using surface pressure and temperature values from ERA-Interim and following the methodology of Bevis et al. (1992, 1994). IWV_{erai} was obtained using the Zenith Wet Delay (ZWD) and mean temperature (T_m) from the ERA-Interim (from GOP-TropDB). Finally, IWV_{erai} was compared to IWV_{gnss} at 6-hourly resolution for 5 years of data. We denote the difference between IWV_{erai} and IWV_{gnss} as ΔIWV (i.e. $\Delta IWV = IWV_{erai} - IWV_{gnss}$) and the correlation coefficient between IWV_{erai} and IWV_{gnss} as r_{iwv}.

Table 4 shows the statistics for ΔIWV and r_{iwv} for the selected stations in each climate zone. The RMS of ΔIWV varies from 0.97 to 11.57 kg/m² whereas the value of r_{iwv} varies from 0.84 to 1.00 between various climate zones. The highest value of r_{iwv} (1.00) has been found for the selected stations in the zones Cwa, Dfc, Dsb, Dwa and Dwb.

Table 4. Statistics of ΔIWV for stations in different climate zones

Zone	Station	Mean [kg/m²]	SDev. [kg/m²]	RMS [kg/m²]	r_{iwv}
Af	PIMO	1.52	3.38	3.70	0.89
Am	KOKB	-0.23	2.45	2.46	0.80
As	ICAM	0.31	3.33	3.34	0.94
Aw	DARW	-0.96	2.92	3.08	0.98
BSh	NICO	0.17	2.47	2.48	0.87
BSk	CEDU	-0.64	1.96	2.06	0.92
BWh	KARR	-0.88	3.05	3.17	0.96
BWk	GOLD	0.89	1.84	2.05	0.87
Cfa	USNO	-0.38	2.89	2.91	0.92
Cfb	DUND	-0.22	1.85	1.87	0.97
Cfc	REYK	0.75	1.29	1.49	0.97
Csa	MATE	-0.02	2.10	2.11	0.90
Csb	JPLM	-0.05	2.46	2.47	0.84
Cwa	UNSA	8.55	7.80	11.57	1.00
Cwb	KUNM	0.38	2.78	2.80	0.89
Dfa	DAEJ	-0.35	2.29	2.32	0.99
Dfb	LAMA	0.75	1.51	1.68	0.97
Dfc	CHUR	0.34	1.15	1.20	1.00
Dsb	BREW	2.53	2.47	3.54	1.00
Dsc	WHIT	-0.19	0.95	0.97	0.99
Dwa	SUWN	-0.49	2.19	2.24	1.00
Dwb	IRKT	-0.03	2.00	2.01	1.00
Dwc	ULAB	0.69	1.36	1.52	0.90
EF	OHI2	-0.36	1.19	1.24	0.86
ET	HOFN	1.15	1.47	1.86	0.95

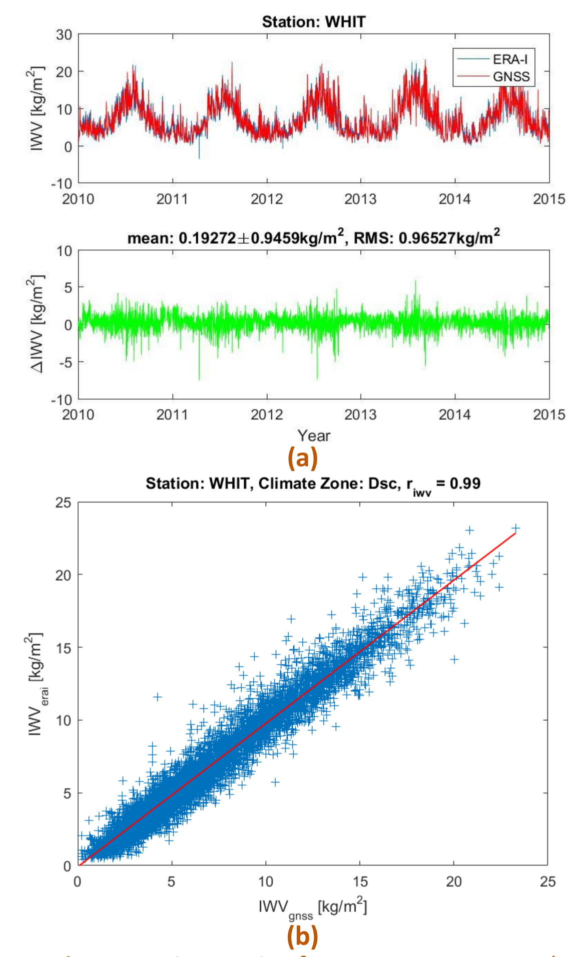

Figure 5. Time series for IWV_{erai}, IWV_{gnss} and ΔIWV, and correlation plot between IWV_{erai} and IWV_{gnss} for station WHIT

Figure 5 shows the IWV time series comparison and correlation for the station WHIT as an example. In terms of IWV, this comparison will be extended to cover all the 400 global stations in the near future.

Conclusions

ZTD derived from the ERA-Interim climate reanalysis model (ZTD_{erai}) was validated for 25 climate zones by a comparison with GNSS-derived ZTD (ZTD_{gnss}) at the locations of over 400 globally distributed (in different climate zones) ground-based GNSS stations. The correlation coefficient (r_{ztd}) between ZTD_{erai} and ZTD_{gnss} was found to be between 0.87 and 1.00 for the various climate zones. The highest value of r_{ztd} (1.00) was found for the three "Cold" climate zones namely Dsc (cold - dry summer - cold summer), Dwa (cold - dry winter - hot summer) and Dwc (cold- dry winter - cold summer), and the second-highest value (0.99) of r_{ztd} was found for another "Cold" climate zone (Dwc or cold- dry winter - cold summer). The lowest value of r_{ztd} (0.87) was found for the "Tropical" climate zone Af (tropical-rainforest) whereas the second-lowest value (r_{ztd} = 0.88) was found for the "Tropical" climate zones As (tropical – dry summer) and Aw (tropical - savannah). These values of the correlation coefficient suggested that the correlation between ZTD_{erai} and ZTD_{gnss} is high in the regions with low amount of atmospheric water vapor and is low in the regions with high amount of atmospheric water vapor.

It was also found that the highest mean, standard deviation and RMS of the differences correspond to the climate zones with high altitude, high topographic variation and high periodicity in the ZTD residuals. Furthermore, a generalization of the global statistics in terms of latitude suggested that the agreement between ZTD_{erai} and ZTD_{gnss} is relatively better towards the polar regions as compared to that in the regions around the equator. This fact reinforced the conclusion that ZTD_{erai} has higher accuracy in the regions with lower amount of atmospheric water vapor.

The correlation coefficient between IWV_{erai} and IWV_{gnss} ranges from 0.84 to 1.00 whereas the RMS agreement varies between 0.97 and 11.57 kg/m² in different climate zones.

References

Bevis, M., S. Businger, Chiswell S., T. A. Herring, R. A. Anthes, C. Rocken, R. H. Ware (1994) GPS Meteorology: Mapping Zenith Wet Delays onto Precipitable Water, Journal of Applied Meteorology, 33(3), 379-386

Bevis, M., S. Businger, T. A. Herring, C. Rocken, R. A. Anthes, and R. H. Ware (1992) GPS Meteorology: Remote Sensing of atmospheric water vapor using the Global Positioning System, Journal of Geophysical Research, 97(D14), 15 787-15 801

Peel, M. C., Finlayson, B. L., and McMahon, T. A. (2007): Updated world map of the Köppen-Geiger climate classification, Hydrol. Earth Syst. Sci., 11, 1633-1644, doi:10.5194/hess-11-1633-2007

Acknowledgements

All the ERA-Interim parameters used in this study have been thankfully obtained from the GOP-TropDB online service (http://www.pecny.cz/gop/index.php/gop-tropdb/tropo-model-service). International GNSS Service, EUREF Permanent Network, RGP and BIGF are thankfully acknowledged for providing the GNSS observation data from their networks. Various products to support GNSS data processing were obtained from IGS and CODE. Furthermore, High Performance Computing (HPC) service of the University of Luxembourg are gratefully acknowledged for support in GNSS data processing.

Download This Poster

Presented at: EGU General Assembly 2017 | 23-28 April 2017 | Vienna, Austria